

Influence of foam initial liquid fraction on the effectiveness of spherical explosion attenuation in a pipe

© R.Kh. Bolotnova, E.F. Gainullina, V.A. Korobchinskaya

Mavlyutov Institute of Mechanics UFRC RAS,
450054 Ufa, Russia
e-mail: elina.gef@yandex.ru

Received April 28, 2024

Revised October 8, 2024

Accepted October 30, 2024

Interaction features of a spherical shock wave formed in the center of a non-deformable pipe filled with gas and contained the protective layer of aqueous foam on its inner surface are investigated. Numerical modeling is carried out on the basis of a two-phase gas-liquid model with a single pressure of phases, taking into account interphase forces and heat transfer. Reliability of the model is confirmed by comparing the calculations with experiments on a spherical explosion in aqueous foam. Pressure evolution on the pipe surface in the near zone of shock wave initiation is analyzed in detail in the absence and presence of foams with different liquid fraction. Significant decrease in the amplitude and velocity of the wave pulse is shown by using foam protection on the pipe wall.

Keywords: aqueous foam, shock waves, cylindrical pipe, numerical simulation.

DOI: 10.61011/TP.2024.12.60426.379-24

Study of aqueous foams damping properties in dynamic loading is important in terms of potential employment of foam barriers as effective protections against impacts. Experimental studies have shown that covering the explosive charge with aqueous foam layer reduces the shock pulse amplitude and propagation velocity [1–4]. A foam barrier placed at a distance from the shock wave (SW) initiation point also reduces the compression wave velocity significantly, which is confirmed by shock-tube experiments [5,6]. It is shown in [1] that, in the case of a strong impact, liquid films that form the foam are destroyed and transform the foam into a gas-droplet mixture. To investigate the dynamics of strong SWs in aqueous foam, the authors proposed a gas-droplet foam model [7–9] that was used to study numerically SW propagation processes in aqueous foam and interaction between a spherical impulse and protective foam barrier.

This work continues the study in [8] that investigated the spherical explosion dynamics in a non-deforming tube containing the aqueous foam layer on the internal surface. Unlike the previous studies, this work addresses in detail the aspects of reduced shock wave intensity on the tube surface in the near zone of spherical explosion initiation depending on the initial liquid fraction of the aqueous foam layer.

SW dynamics in gas (nitrogen) and aqueous foam was described using the following conservation equations for a two-phase single-pressure gas-liquid mixture model in two-velocity and two-temperature approximations taking into account the interphase heat transfer and interphase interaction forces [10,11]:

Phase continuity equations

$$\frac{\partial(\alpha_i \rho_i)}{\partial t} + \text{div}(\alpha_i \rho_i \mathbf{v}_i) = 0.$$

Phase momentum equations

$$\begin{aligned} \frac{\partial(\alpha_i \rho_i \mathbf{v}_i)}{\partial t} + \text{div}(\alpha_i \rho_i \mathbf{v}_i \mathbf{v}_i) &= -\alpha_i \nabla p \\ &+ \text{div}(\alpha_i \boldsymbol{\tau}_i) + \mathbf{F}_{i,drag} + \mathbf{F}_{i,vm}. \end{aligned}$$

Phase energy equations

$$\begin{aligned} \frac{\partial(\alpha_i \rho_i E_i)}{\partial t} + \text{div}(\alpha_i \rho_i E_i \mathbf{v}_i) &= -p \frac{\partial \alpha_i}{\partial t} - \text{div}(\alpha_i \mathbf{v}_i p) \\ &+ \text{div}(\alpha_i \frac{c_{p,i}}{c_{v,i}} \gamma_i \nabla h_i) + K_{ht}(T_j - T_i) + \text{div}(\alpha_i \mathbf{v}_i \cdot \boldsymbol{\tau}_i). \end{aligned}$$

Equation of the water volume fraction dynamics in the foam layer

$$\begin{aligned} \frac{\partial \alpha_1}{\partial t} + \text{div}(\alpha_1 \mathbf{v}) + \text{div}(\alpha_1 \alpha_2 (\mathbf{v}_1 - \mathbf{v}_2)) \\ - \alpha_1 \text{div} \mathbf{v} = \alpha_1 \alpha_2 \left(\frac{1}{\rho_2} \frac{d\rho_2}{dt} - \frac{1}{\rho_1} \frac{d\rho_1}{dt} \right). \end{aligned}$$

Here, p is the pressure, α_i is the volume fraction, ρ_i is the density, \mathbf{v}_i is the velocity, $\boldsymbol{\tau}_i = \mu_i (\nabla \mathbf{v}_i + \nabla \mathbf{v}_i^T) - \frac{2}{3} (\mu_i \text{div} \mathbf{v}_i) \mathbf{I}$ is the viscous stress tensor, μ_i is the dynamic viscosity, \mathbf{I} is the unit tensor, $\mathbf{F}_{i,drag}$ is the interphase drag force determined by the Schiller–Naumann model, $\mathbf{F}_{i,vm}$ is the virtual mass force, $E_i = e_i + K_i$ is the total energy, e_i is the internal energy, K_i is the kinetic energy, $c_{p,i}$, $c_{v,i}$ are specific heat capacities at constant pressure and volume, γ_i is the thermal diffusivity, h_i is the enthalpy, K_{ht} is the Ranz–Marshall interphase heat transfer intensity, T_i is the temperature, $\mathbf{v} = \alpha_1 \mathbf{v}_1 + \alpha_2 \mathbf{v}_2$ is the gas-liquid mixture velocity. Subscripts i , $j = 1, 2$ refer to the water and gas phases, respectively. The Peng–Robinson equation of state was used to describe thermodynamic properties of nitrogen. Water was described

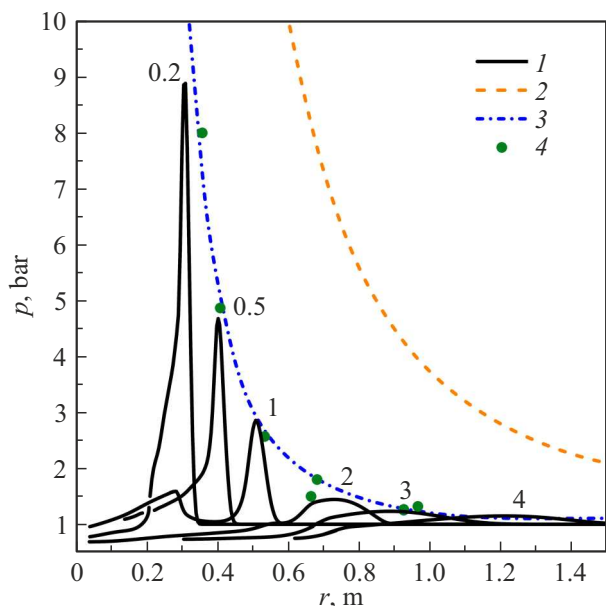


Figure 1. Calculated pressure profiles (*1*) at the specified times (ms); 2, 3 — summarized experimental data on maximum pressures in SW during the spherical explosion in gas (2) [14] and aqueous foam (3) [15]; 4 — peak pressures in spherical explosion experiments in foam with $\alpha_{10} = 0.0083$ [1].

by the equation of state that was linear in temperature and density [12].

The model implies that foam behind the strong SW front is broken into microdrops [13] in the form of monodisperse gas-drop mixture.

Implementation of the proposed gas-liquid model was performed using a solver developed by the authors on the basis of the twoPhaseEulerFoam solver in OpenFOAM software [12]. When constructing the computational domain for numerical simulation, the multiblock grids were generated, which characterized by cell thickening in the explosion initiation area. Grid convergence of the obtained results was controlled by stage grid refinement as well as by varying pre-defined accuracy parameters of the PIMPLE iteration algorithm until solution stability is achieved. The best accuracy and stability were achieved at the following

grid domain discretization parameters: $\Delta t = 1 \cdot 10^{-10}$ s; $\Delta x, \Delta y = 0.001-0.003$ m. The Euler and Gauss schemes were used for derivative approximation in time and space.

To estimate the model consistency and numerical implementation method, a comparative analysis of calculations and experimental data by the maximum pressures was performed [1] for the problem of spherical explosion in aqueous foam with the liquid volume fraction $\alpha_{10} = 0.0083$ (Figure 1). Initial pressure pulse distribution during explosion was set as

$$p(0, x, y, z) = p_0 + \Delta p \exp(-(x^2 + y^2 + z^2)/a^2), \quad (1)$$

where $\Delta p = 3000$ MPa, $p_0 = 0.1$ MPa, $a = 0.035$ m.

Figure 1 additionally shows the generalized experimental peak pressures in gas [14] and aqueous foam [15] that demonstrate significant SW intensity attenuation in foam. A satisfactory agreement between the calculations and experiments was achieved [1,15].

When solving the main problem the spherical explosion was simulated in the center of undeformed cylindrical tube with the radius $r = 1.4$ m filled with nitrogen and containing a 0.4 m foam layer for the initial liquid volume fraction of foam $\alpha_{10} = 0, 0.1, 0.15, 0.2$. Initial pulse parameters set as (1) are as follows: $\Delta p = 100$ MPa, $p_0 = 0.1$ MPa, $a = 0.15$ m.

First, SW dynamics was calculated in conditions without a foam layer inside the tube. Typical pressure isolines (bar) at the specified times are shown in Figure 2.

By $t = 1.1$ ms, SW reaches the tube’s rigid boundary, and after reflection from it, the pressure amplitude on the wall grows up to 9.6 bar at $t = 1.2$ ms. Then, the high pressure zone is shifted and attenuated ($p \approx 3$ bar at $t = 2$ ms, $p \approx 2.4$ bar at $t = 4$ ms). Formation of a low pressure zone ($p \approx 0.9$ bar, $t = 2$ ms) is observed near the symmetry axis. Further interaction between the wave pulses and side surface of the tube and on the symmetry axis induces a low pressure area near the tube wall ($p \approx 0.5$ bar, $t = 4$ ms).

Figure 3 shows the calculated pressure field distributions at times corresponding to the most intense impact on the tube wall for the specified initial liquid fractions of the foam layer.

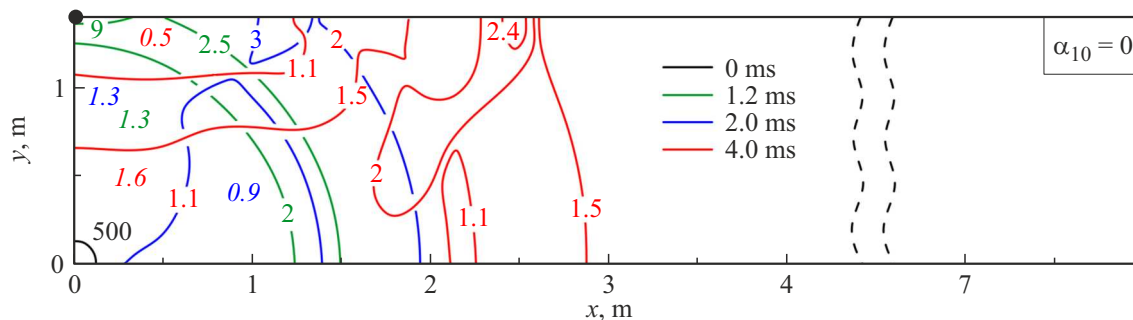


Figure 2. Calculated pressure isolines with indicated values (bar) at the specified times during the spherical explosion in a gas-filled tube. Italics — typical pressures inside the zones confined by isobars. Pressure dynamics test point: $x = 0, y = 1.4$ m (see Figure 4).

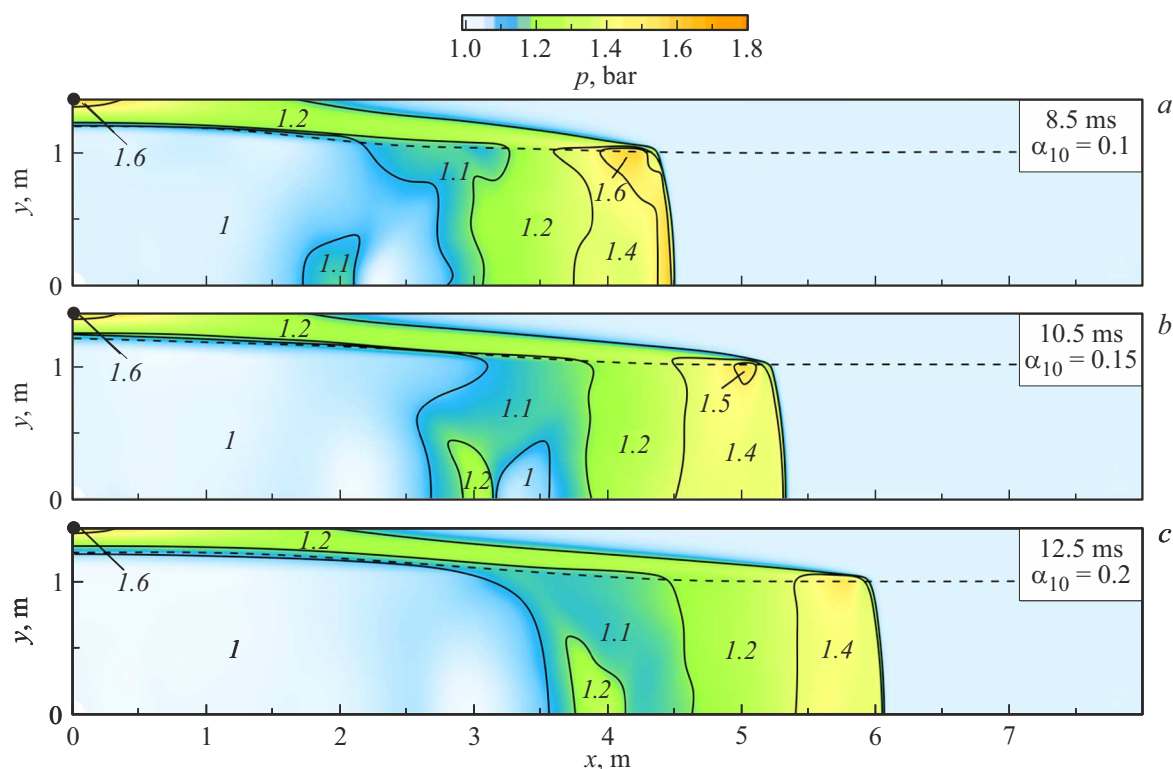


Figure 3. Calculated pressure field distributions at times (ms) for α_{10} in the aqueous foam layer on the internal surface of the gas-filled tube. Italics — typical pressures inside the zones confined by isobars. Pressure dynamics test point: $x = 0, y = 1.4$ m (see Figure 4). Dashed line — foam layer boundary.

During interaction with the pressure pulse, aqueous foam compaction leads to significant reduction of the foam velocity. Typical time of maximum SW pressure achievement on the tube surface without a foam layer ($\alpha_{10} = 0$) is $t \approx 1.2$ ms. For $\alpha_{10} = 0.1$ of the foam layer, this time increases by a factor of ~ 7 ($t \approx 8.5$ ms); for $\alpha_{10} = 0.15$ — by a factor of ~ 9 ($t \approx 10.5$ ms), and for $\alpha_{10} = 0.2$ — by a factor of ~ 10 ($t \approx 12.5$ ms). The specified times show the numerical estimate of the pressure pulse propagation rate in the foam layer depending on its water content compared with compression pulse propagation in a tube without foam protection (Figure 2, 3).

Calculated time dependences of pressure amplitude in the point of tube $x = 0, y = 1.4$ m, located at the minimum distance from the point of explosion (Figure 2, 3) are shown in Figure 4. Maximum pressures recorded on the tube surface with the foam layer are ~ 1.7 bar, which is ~ 5 times as low as those in the given zone $x = 0, y = 1.4$ m without a foam layer.

The numerical analysis has shown that an impact on a tube wall without foam protection has an oscillating nature induced by re-reflection of pressure pulses that are formed during interaction of the principal wave and reflected waves from the tube surface with the symmetry axis. The amplitude of secondary pulses on the tube wall exceeds the corresponding maximum pressures with the presence of the foam layer (compare lines 1–4 in Figure 4). Degrees

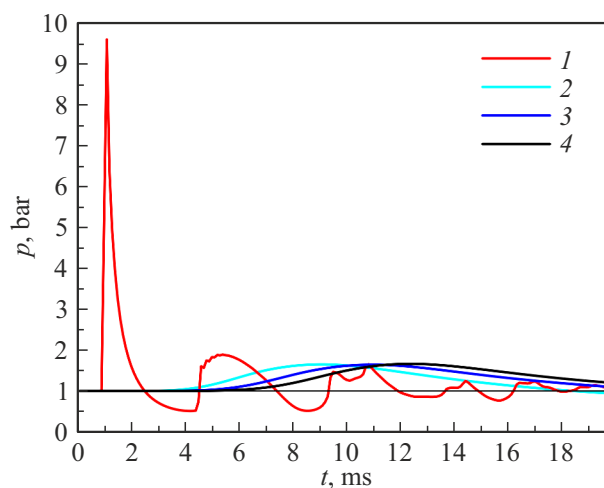


Figure 4. Calculated dependences of the pressure amplitude on time at the tube boundary closest to the point of explosion ($x = 0, y = 1.4$ m, see Figure 2, 3): 1 — calculations at $\alpha_{10} = 0$; 2–4 — calculations with the presence of foam protection on the internal surface of the tube with $\alpha_{10} = 0.1, \alpha_{10} = 0.15$ and $\alpha_{10} = 0.2$, respectively.

of compression pulse rate and amplitude reduction when the pulse propagates in the foam layer were estimated depending on the increase in the initial water content in the foam layer.

The results present details of the aspects of wave processes that take place in the tube with an aqueous foam barrier that lead to significant reduction of pressure pulse intensity and rate when the pressure pulse interacts with the tube boundary compared with the case without a foam protection, which facilitates tube damage risk mitigation during an internal explosion. The investigations may be used, in particular, to develop safety methods for gas pipeline transportation.

Funding

The work was supported by state budget funds under state task 124030400064-2 (FMRS-2024-0001).

Conflict of interest

The authors declare no conflict of interest.

References

- [1] E. Del Prete, A. Chinnayya, L. Domergue, A. Hadjadj, J.-F. Haas. *Shock Waves*, **23** (1), 39 (2013). DOI: 10.1007/s00193-012-0400-0
- [2] S.P. Medvedev, S.V. Khomik, V.N. Mikhalkin, A.N. Ivantsov, G.L. Agafonov, A.A. Cherepanov, T.T. Cherepanova, A.S. Betev. *J. Phys.: Conf. Ser.*, **946**, 012061 (2018). DOI: 10.1088/1742-6596/946/1/012061
- [3] K.L. Monson, K.M. Kyllonen, J.L. Leggitt, K.E. Edmiston, C.R. Justus, M.F. Kavlick, M. Phillip, M.A. Roberts, C.W. Shegogue, G.D. Watts. *J. Forensic Sci.*, **65** (6), 1894 (2020). DOI: 10.1111/1556-4029.14536
- [4] K. Ahmed, A.Q. Malik. *AIP Advances*, **10**, 065130 (2020). DOI: 10.1063/5.0010283
- [5] G. Jourdan, C. Mariani, L. Houas, A. Chinnayya, A. Hadjadj, E. Del Prete, J.-F. Haas, N. Rambert, D. Counilh, S. Faur. *Phys. Fluids*, **5**, 056101 (2015). DOI: 10.1063/1.4919905
- [6] M. Monloubou, J. Le Clanche, S. Kerampran. *Actes 24eme Congres Francais de Mecanique*. Brest: AFM, 255125 (2019).
- [7] E.F. Gainullina. *Multiphase systems*, **14**(2), 74 (2019) (in Russian). DOI: 10.21662/mfs2019.2.011
- [8] R.Kh. Bolotnova, E.F. Gainullina. *Bulletin of the South Ural State University. Seriya „Matematicheskoe modelirovanie i programmirovaniye“*, **14** (1), 118 (2021) (in Russian). DOI: 10.14529/mmp210109
- [9] R.Kh. Bolotnova, E.F. Gainullina, V.A. Korobchinskaya. *Tech. Phys. Lett.*, **12**, 104 (2023).
- [10] R.I. Nigmatulin. *Dynamics of multiphase media* (Hemisphere, NY, 1990)
- [11] L.D. Landau, E.M. Lifshitz. *Fluid mechanics* (Pergamon Press, Oxford, 1987), v. 6.
- [12] Electronic source. *OpenFOAM. The open source computational fluid dynamics (CFD) toolbox*. Available at: <http://www.openfoam.com>
- [13] S.A. Zhdan. *FGV*, **26** (2), 103 (1990) (in Russian). <https://elibrary.ru/item.asp?id=30555610>
- [14] G. Kinney, K. Graham. *Explosives shocks in Air* (Springer, Berlin, 1985)
- [15] W. Hartman, B. Boughton, M. Larsen. *Blast mitigation capabilities of aqueous foam* (Sandia National Laboratories Tech. Rep. SAND2006–0533, 2006), p. 98.

Translated by E.Ilinikaya